



An enhanced numerical procedure for the shakedown analysis in multidimensional loading domains



K.V. Spiliopoulos^{a,*}, K.D. Panagiotou^{b,c}

^a Institute of Structural Analysis & Antiseismic Research, Department of Civil Engineering, National Technical University of Athens, Zografou Campus, 157-80 Athens, Greece

^b AICES, RWTH Aachen University, Schinkelstraße 2, 52062 Aachen, Germany

^c Institute of Applied Mechanics, RWTH Aachen University, Mies-van-der-Rohe-Straße 1, 52074 Aachen, Germany

ARTICLE INFO

Article history:

Received 6 June 2017

Accepted 15 August 2017

Keywords:

Numerical algorithms

Direct methods

Cyclic loading

Plasticity

Shakedown

Residual stresses

ABSTRACT

The Residual Stress Decomposition Method for Shakedown (RSDM-S) is a new iterative direct method to estimate the shakedown load in a 2-dimensional (2D) loading domain. It may be implemented to any existing finite element code, without the need to use a mathematical programming algorithm. An improved and enhanced RSDM-S is proposed herein. A new convergence criterion is presented that makes the procedure almost double as fast. At the same time, the procedure is formulated in a 3-dimensional (3D) polyhedral loading domain, consisting of independently varying mechanical and thermal loads. Using a cyclic loading program that follows the outline of this domain, it is shown that there is hardly any increase in the computational time when passing from a 2D to a 3D domain. Finally, keeping the efficiency, using an alternative cyclic loading program, an automation of the approach to any n-dimensional loading domain is presented. Examples of application are included.

© 2017 Elsevier Ltd. All rights reserved.

1. Introduction

A major task in civil and mechanical engineering is the estimation of the load carrying capacity of a structure or a component under variable loadings. Structures, like buildings, bridges, pavements, nuclear reactors, aircraft propulsion engines, etc., during their lifetime, are subjected to loads (live load, heavy traffic, seismic action, internal pressure, thermo-mechanical loads, etc.) acting in a varying manner. This type of cyclic mechanical and thermal loading leads often these structures beyond the elastic limit, resulting to plastic straining.

The asymptotic cyclic behavior of an elastic-perfectly plastic structure under cyclic loading may be determined by time consuming incremental time-stepping calculations. Direct methods, alternatively, have a big computational advantage as they attempt to find directly this cyclic asymptotic state. Such states are guaranteed for structures made of stable material [1].

There are a few direct methods, proposed in the literature, among which one may mention the work presented in [2,3] which forms a sequence of elastic solutions using as a modified loading an update of initial strains computed through an update of internal variables. This method is the basis of a recently presented direct

method [4]. Approaches based also on a series of elastic analyses produced by modifying, iteratively, the modulus of elasticity, form another class of direct methods. Among them one should mention the Linear Matching Method (LMM) [5,6]. An incremental-iterative procedure, that appears to work well in cases of alternative plasticity but not for cases of ratcheting, was proposed in [7] and has been implemented in a commercial code. Very recently, a numerical scheme is presented, based on the conditions of the asymptotic state linked with a specific trial and projection operation, to estimate the plastic strain increments [8].

A direct method, which is known as the Residual Stress Decomposition Method (RSDM), was presented in [9,10]. The method can predict the long-term cyclic state, either it is shakedown or reverse plasticity or incremental collapse, of an elastic perfectly-plastic structure when subjected to a given cyclic loading history. The approach is based on physical arguments that have to do with the expected cyclic nature of the residual stresses. The residual stresses are decomposed into Fourier series with respect to time and the coefficients of these series are calculated iteratively by satisfying equilibrium and compatibility at time points inside the cycle.

When, on the other hand, the loading history is unknown, for a structure to be safe and serviceable, safety margins, e.g. shakedown limits, have to be estimated so that it fails neither due to incremental collapse (often referred to as ratcheting) nor due to reverse plasticity that leads to low cycle fatigue. A direct

* Corresponding author.

E-mail address: kvspilio@central.ntua.gr (K.V. Spiliopoulos).

shakedown analysis is the only way to provide this information. For small displacements and elastic-perfectly plastic solids the shakedown analysis is based on two different approaches, the lower bound [11] or the upper bound [12] shakedown theorems. The extensions of these two theorems to cover thermal loadings were given in [13,14], respectively.

Attempts to consider geometric nonlinearities appeared in the literature (e.g. [15,16]). Conditions to extend the static theorem to elastic-perfectly plastic cracked bodies have been presented in [17]. Limited kinematic (e.g. [18]) and nonlinear kinematic hardening has been also addressed (e.g. [19]). Recent developments on the subject have appeared in [20,21] in the framework of the bipotential theory. Non-associated plasticity has also been discussed (e.g. [22,23]). Polizzotto, has discussed the shakedown theorems in the context of gradient plasticity theory [24,25].

The two shakedown theorems form the basis of the big majority of the existing numerical procedures to estimate the shakedown load. They are formulated as mathematical programming (MP) problems whose scope is to find the minimum or maximum value of an objective function (normally the loading factor) which is subjected to various static or kinematic constraints. Linearization, mainly of the yield surface, has led to some early solutions using linear programming algorithms (e.g. [26,27]). More recent contributions have appeared along the same line (e.g. [28–30]). If the constraints are not linearized and are kept in their original form (nonlinear), the problem can be formulated as a nonlinear (NLP) programming problem. The discretization of the continuum by a large number of finite elements and the big number of constraints often lead to the solution of large size optimization problems. Various numerical techniques have been developed to solve these problems. Among these one could mention the reduced basis technique [19,31] or algorithms based on Newton iterations [32]. The evolution of the interior point algorithms (IPM) to solve large scale optimization problems led to the extensive formulation and solution of limit and shakedown analysis problems using these algorithms or related techniques (e.g. [33–43]).

One may also find some alternative approaches in the literature for the evaluation of the shakedown load. Such an approach is based on the work presented in [2], whose application using the finite element method (FEM) may be found in subsequent publications (e.g. [44]). Reverse plasticity and collapse load solutions have been shown to provide upper bounds to the shakedown load [45]. The LMM has also been used to estimate the shakedown load of a structure (e.g. [5,46]). In [47] a solution is proposed, based on the LMM, to estimate a possible shakedown load when friction slip occurs between a rigid surface in contact with an elastic body, subjected to cyclic loading. A quite involved strategy, equivalent to a fictitious incremental strain driven elastoplastic problem, and applied for a von Mises type of material, has been presented in [48]. The numerical performance of this approach is compared against the IPMs in [49]. An analogous methodology, involving more general yield criteria, was proposed in [50].

A numerical approach, which was called RSDM-S has appeared recently [51–53]. It may be used for the evaluation of the shakedown load of elastic-perfectly plastic structural elements under cyclic thermo-mechanical loading. The basis of the method, both from the conceptual as well as the implementation points of view, is the RSDM. Since, now, only the variation intervals of the loads are known, the problem is converted to an equivalent prescribed loading problem, drawing any time curve crossing these intervals. The RSDM-S consists of two different iteration loops, one inside the other and has been formulated for two loads that may vary either proportionally or independently. Starting from a high load factor, a descending sequence of loading factors is established and the shakedown load factor is calculated when the iterative procedure

converges to a solution where the constant term is the only non-zero term of the Fourier series.

The efficiency of the RSDM-S and RSDM to provide shakedown boundaries as well as to unveil unsafe conditions in 2-dimensional loading domains was recently demonstrated in [54].

In the present work, the RSDM-S method is enhanced by a different convergence criterion, inside the inner loop, that makes the method run faster, even more than 40%. Moreover, the method is formulated for a 3-dimensional loading domain consisting of two mechanical and a thermal load. It is shown that the extension from a 2-D to a 3-D loading domain hardly influences the amount of computational time to estimate the shakedown load factor as opposed to the IPM algorithms where the time is shown to double [55]. Finally, it is shown how the method may be automated to cater for any n-dimensional loading domain.

The paper is organized in the following way: In Section 2 a proof of an existing theorem makes possible to realize the arbitrariness of the cyclic loading program that passes through the vertices of the convex loading domain; in Section 3 the enhanced RSDM-S procedure, in the form of a flow chart, with the new convergence criterion, formulated in a 3-D thermomechanical loading domain and assuming a von Mises yield criterion, is presented. The significant faster convergence of the enhanced approach is demonstrated through examples of 2-D loading domains in Section 4. In Section 5 the method is applied to a 3-D polyhedral loading domain using a cyclic loading program that passes consecutively from all its vertices. Finally, in Section 6 an alternative cyclic loading path combined with a combinatorial algorithm shows how the whole procedure may be automated for an n-dimensional domain.

2. Theoretical considerations

Let us suppose a structure is subjected to independently varying cyclic loads that have the same period T . Although the theory may be applied to any number of loads, for reasons of visualization, a maximum of three loading (3-D) domain that consists of two mechanical and a thermal load will be demonstrated (Fig. 1(a)). Such a cyclic loading may be represented in the loading space as a closed loop (Fig. 1(b)). Let us further suppose that each load has a minimum and a maximum value of variation. Without any loss of generality, the minimum of all the loads will be considered zero. The maximum of each of the loads, denoted by starred quantities, together with the origin may define a convex (hyper-) cuboid (Fig. 1(b)). Thus, the cyclic loading will be contained inside this cuboid.

In response to this loading the structure that consists of an elastic-perfectly plastic material will develop a stress that may be decomposed into two parts; an elastic part assuming purely elastic material behavior and a residual stress part to account for plasticity:

$$\boldsymbol{\sigma}(\tau) = \boldsymbol{\sigma}^{el}(\tau) + \boldsymbol{\rho}(\tau) \quad (1)$$

where $\tau = t/T$ denotes a time point inside the cycle.

The structure is discretized, following a standard procedure, into a finite number of elements that are interconnected at a discrete number of nodal points situated on their boundaries. Bold letters are herein used for vectors and matrices. The stress and strain vectors are evaluated at the Gauss points (GPs) of the finite elements (FE).

The strain rates, on the other hand, may be decomposed into the following parts:

$$\dot{\boldsymbol{\epsilon}}(\tau) = \dot{\boldsymbol{\epsilon}}^{el}(\tau) + \dot{\boldsymbol{\epsilon}}^{\theta}(\tau) + \dot{\boldsymbol{\epsilon}}_r^{el}(\tau) + \dot{\boldsymbol{\epsilon}}^{pl}(\tau) \quad (2)$$

where $\dot{\boldsymbol{\epsilon}}^{el}(\tau)$ is the elastic straining due to both the mechanical and the thermal loading [52]. $\dot{\boldsymbol{\epsilon}}^{\theta}(\tau)$ denotes thermal strain rates that

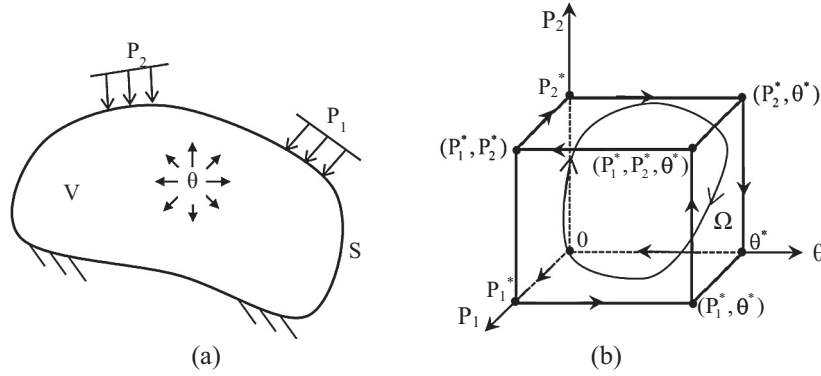


Fig. 1. (a) Structure with applied thermomechanical loads, (b) 3-D loading domain.

may be calculated from the temperature distribution using the coefficient of thermal expansion. The last two parts of (2) come from the inelastic behavior with the very last one being the plastic strain rate vector.

The following relations may be written between strains and stresses:

$$\begin{aligned} \dot{\sigma}^{el}(\tau) &= \mathbf{D} \cdot \dot{\epsilon}^{el}(\tau) \\ \dot{\rho}(\tau) &= \mathbf{D} \cdot \dot{\epsilon}_r^{el}(\tau) \\ \dot{\epsilon}^{pl}(\tau) &= \dot{\lambda} \frac{\partial f}{\partial \sigma(\tau)} \end{aligned} \quad (3)$$

with f being a convex yield surface, containing the stresses' origin, and $\dot{\lambda}$ the plastic multiplier and \mathbf{D} the material matrix.

A stress state may be either inside or on the yield surface. A state of stress σ inside the yield surface is a safe stress for which $f(\sigma) < 0$, whereas if it is either on the yield surface or inside is an allowable stress state for which $f(\sigma) \leq 0$.

For two stress states σ, \mathbf{q} one may write the following inequality due to the convexity of the yield surface [56]:

$$f(\beta\sigma + (1 - \beta)\mathbf{q}) \leq \beta f(\sigma) + (1 - \beta)f(\mathbf{q}) \quad (4)$$

where $0 \leq \beta \leq 1$.

Since $\mathbf{q} = \mathbf{0}$ is a safe state of stress one may write:

$$f(\beta\sigma) \leq \beta f(\sigma) \quad (5)$$

where for a homogeneous yield function f , as, for example, a von Mises yield criterion, equality holds.

Also, related to the convexity of the yield surface is the Drucker's postulate of stability [1]. In [57] it is proved that a structure whose material obeys Drucker's postulate will reach, after many cycles of loading, an asymptotic state in which the stresses and strain rates gradually stabilize and become also cyclic having the same period with the applied loads [58].

Shakedown is a favorable asymptotic state such that, provided the load margins are below a threshold, the structure adapts itself, after some initial plastic straining, to a purely elastic behavior. Conditions for shakedown are given by Melan's theorem [11]. The theorem is composed of the following two statements [59]:

- (a) The structure will shake down under a cyclic loading if there exists a time-independent distribution of residual stresses $\bar{\rho}$ such that, under any combination of loads inside prescribed limits, its superposition with the elastic stresses σ^{el} , i.e. $\sigma^{el} + \bar{\rho}$, results in a total safe stress state at any point of the structure,
- (b) Shakedown never takes place unless a time-independent distribution of residual stresses can be found such that, under all the possible load combinations, the sum of the residual and elastic stresses constitutes an allowable stress state.

The following theorem is useful in the numerical investigation for the shakedown threshold [60]:

"If a structure shakes down under a cyclic loading containing all the vertices of the convex loading domain Ω then it shakes down for any loading path contained in Ω ".

A proof, which highlights some important issues, is presented next:

Let us consider a stress point at some cyclic loading path inside the convex domain. We may write the elastic solution at this point as a linear combination [61] of the elastic solutions at its vertices:

$$\sigma^{el} = \beta_1 \sigma_1^{el} + \beta_2 \sigma_2^{el} + \dots + \beta_s \sigma_s^{el} \quad (6)$$

where $\beta_1 + \beta_2 + \dots + \beta_s = 1$ and $\beta_i \geq 0$, with $i = 1, \dots, s$, where s is the number of vertices of the convex loading domain, and σ_i^{el} are the elastic stresses at each vertex of this domain.

Since by the hypothesis, a cyclic loading that passes through the vertices of the loading domain at different time points causes the structure to shake down, according to Melan's theorem, a residual stress $\bar{\rho}$ constant in time, and therefore common at all the vertices, will exist, such that the total stress at each vertex will be a safe state of stress:

$$f(\sigma_i^{el} + \bar{\rho}) < 0, \quad i = 1, \dots, s \quad (7)$$

This residual stress may be combined with σ^{el} to give:

$$\begin{aligned} f(\sigma^{el} + \bar{\rho}) &= f(\beta_1 \sigma_1^{el} + \beta_2 \sigma_2^{el} + \dots + \beta_s \sigma_s^{el} + \bar{\rho}) \\ &= f[\beta_1 \sigma_1^{el} + \beta_2 \sigma_2^{el} + \dots + \beta_s \sigma_s^{el} + (\beta_1 + \beta_2 + \dots + \beta_s) \bar{\rho}] \end{aligned} \quad (8)$$

using the first property of the coefficients β_i ($\sum_{i=1}^s \beta_i = 1$).

By grouping them, one can write the above expression as:

$$\begin{aligned} f(\sigma^{el} + \bar{\rho}) &= f[\beta_1(\sigma_1^{el} + \bar{\rho}) + \beta_2(\sigma_2^{el} + \bar{\rho}) + \dots + \beta_s(\sigma_s^{el} + \bar{\rho})] \\ &\leq \beta_1 f(\sigma_1^{el} + \bar{\rho}) + \beta_2 f(\sigma_2^{el} + \bar{\rho}) + \dots + \beta_s f(\sigma_s^{el} + \bar{\rho}) \end{aligned} \quad (9)$$

The above inequality is justified through the use of the generalized form of the convexity inequality (4), often called Jensen's inequality, which may be proved by induction. Thus, we conclude:

$$\Rightarrow f(\sigma^{el} + \bar{\rho}) < 0 \quad \text{Q.E.D.} \quad (10)$$

where use of the inequalities (7) and the non-negative nature of the β_i was made.

A 2-D dimensional loading cuboid is a rectangle, i.e. $s = 4$ (2^2). For a 3-D loading domain (Fig. 1(b)), $s = 8$ (2^3). For an n -dimensional loading domain (n -cuboid) one can envisage that the number of vertices will be equal to the combination of the loads in all possible ways. Thus, one may write:

$$s = \binom{n}{0} + \binom{n}{1} + \dots + \binom{n}{k} + \dots + \binom{n}{n} = \sum_{k=0}^n \binom{n}{k} = 2^n \quad (11)$$

where $\binom{n}{k} = \frac{n!}{k!(n-k)!}$ is the binomial coefficient and the expression above is a standard binomial formula that may be found in any mathematics handbook (e.g. [62]).

The construction of a prescribed cyclic loading program that may pass through the vertices of the 3-D loading domain may be seen in Fig. 2. We may see inside one period T the time variation of the three loads that follow the consecutive movements from each vertex to the next (Fig. 1(b)): $0 \rightarrow P_1^* \rightarrow (P_1^*, \theta^*) \rightarrow (P_1^*, P_2^*, \theta^*) \rightarrow (P_1^*, P_2^*) \rightarrow P_2^* \rightarrow (P_2^*, \theta^*) \rightarrow \theta^* \rightarrow 0$. The loading vector may thus be expressed, through its maximum values:

$$\mathbf{P}(\tau) = \begin{Bmatrix} P_1(\tau) \\ P_2(\tau) \\ \theta(\tau) \end{Bmatrix} = \begin{Bmatrix} P_1^* \cdot \alpha_1(\tau) \\ P_2^* \cdot \alpha_2(\tau) \\ \theta^* \cdot \alpha_3(\tau) \end{Bmatrix} \quad (12)$$

where the α_i denote time functions.

3. An enhanced RSDM-S procedure

The RSDM-S [51] has its roots in the RSDM [9] which is a direct method that can be used to determine the kind of asymptotic cyclic state (ratcheting, or reverse plasticity, or shakedown) for a given cyclic history, without following cumbersome time-stepping calculations.

The main idea of the RSDM is to decompose the sought cyclic residual stresses in the asymptotic cycle to Fourier series (13),

$$\rho(\tau) = \frac{1}{2} \mathbf{a}_0 + \sum_{k=1}^{\infty} \{ \cos(2k\pi\tau) \cdot \mathbf{a}_k + \sin(2k\pi\tau) \cdot \mathbf{b}_k \} \quad (13)$$

Differentiating (13) with respect to time, one may get an expression for their derivatives:

$$\dot{\rho}(\tau) = 2\pi \left\{ \sum_{k=1}^{\infty} (-k \sin(2k\pi\tau) \cdot \mathbf{a}_k + k \cos(2k\pi\tau) \cdot \mathbf{b}_k \right\} \quad (14)$$

It is proved that the Fourier coefficients $\mathbf{a}_k, \mathbf{b}_k, \mathbf{a}_0$ may be found in an iterative way through the evaluation of these derivatives. This evaluation is performed by satisfying, at cycle time points, equilibrium, with zero loads, and compatibility [9].

Focusing now on shakedown, the two statements of Melan's theorem define, for a prescribed cyclic loading, the limit cycle which is a transition cycle between one with plastic straining and one without plastic straining. It may be proved [59] that the residual stress distribution of this cycle is unique, being independent of the preceding deformation history.

The numerical procedure RSDM-S is actually an iterative transition process to this cycle. In every iteration (μ) the loading domain

(Fig. 1(b)), and in effect the cyclic loading program (Fig. 2), is multiplied by a loading factor $\gamma^{(\mu)}$. This may be accounted for in the purely elastic part of eqns. (1) and (2), which may now be written as:

$$\sigma(\tau) = \gamma^{(\mu)} \sigma^{el}(\tau) + \rho(\tau) \quad (15)$$

$$\dot{\epsilon}(\tau) = \gamma^{(\mu)} (\dot{\epsilon}^{el}(\tau) + \dot{\epsilon}^{\theta}(\tau)) + \dot{\epsilon}_r^{el}(\tau) + \dot{\epsilon}^{pl}(\tau) \quad (16)$$

With an initial high value, the load factor is sequentially decreased by shrinking the loading domain in a continuous way, until the conditions of the limit cycle are reached [51].

The decomposition of the residual stresses in Fourier series of Eq. (13) provides a natural way to implement the transition to the limit cycle. Thus, the ending phase of the procedure is when, in the course of iterations, the only remaining terms of the Fourier series are the constant terms \mathbf{a}_0 .

As a starting point for the procedure one can use the cycle time point, where one of the loads attains its maximum value, whereas the others are zero (e.g. τ^* in Fig. 2). Having assumed a von Mises type of material, the effective stresses of the elastic stresses corresponding to this load value (P_1^*) at all the GPs may be calculated; the ratio of the uniaxial yield stress σ_Y to the minimum non-zero of these effective stresses may serve as an initial load factor $\gamma^{(1)}$ since this selection, guarantees, at least for this cycle time, that all the elements of the structure will be plastic, rendering $\gamma^{(1)}$ not only far above the shakedown but even the limit load factor [51].

The flow chart of the suggested procedure may be seen in Fig. 3. As one may realize, it consists of two iterative loops one inside the other. The Greek letters κ and μ are used to denote an iteration of the inner and the outer loop respectively. They both have 1 as the initial values.

At an iteration κ a total stress is found that consists of an existing estimate of the residual stresses together with the multiplied by the current loading factor elastic stresses, which are evaluated from the contributions of the two mechanical and the thermal load. If more loads act on the structure they could be easily accommodated here. For the thermal load, in particular, the stresses are calculated using (17)

$$\sigma_{\theta^*}^{el} = \mathbf{D} \cdot \mathbf{B} \cdot \mathbf{r}_{\theta^*} - \mathbf{D} \cdot \mathbf{e}^{\theta^*} \quad (17)$$

where \mathbf{r}_{θ^*} is the vector of nodal displacements due to the peak of the thermal load that may be calculated from (18), with \mathbf{B} being the strain-displacement compatibility matrix in a FE environment and \mathbf{K} being the standard stiffness matrix:

$$\mathbf{K} \cdot \mathbf{r}_{\theta^*} = \int_V \mathbf{B}^T \cdot \mathbf{D} \cdot \mathbf{e}^{\theta^*} dV \quad (18)$$

where the thermal strains \mathbf{e}^{θ^*} , in (17) and (18), are calculated proportional to the temperature θ^* , through the coefficient of thermal expansion.

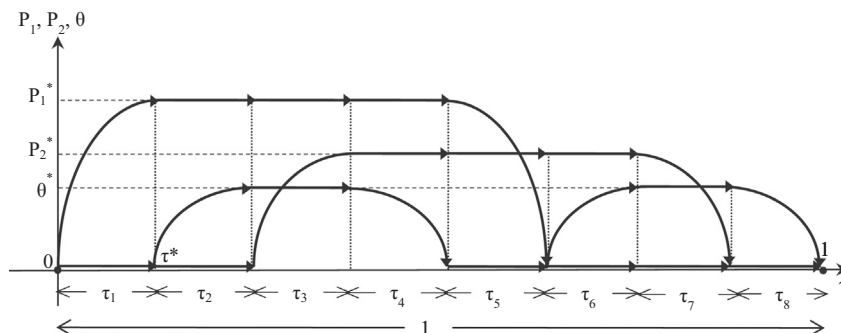


Fig. 2. Individual cyclic load variation over one time period.

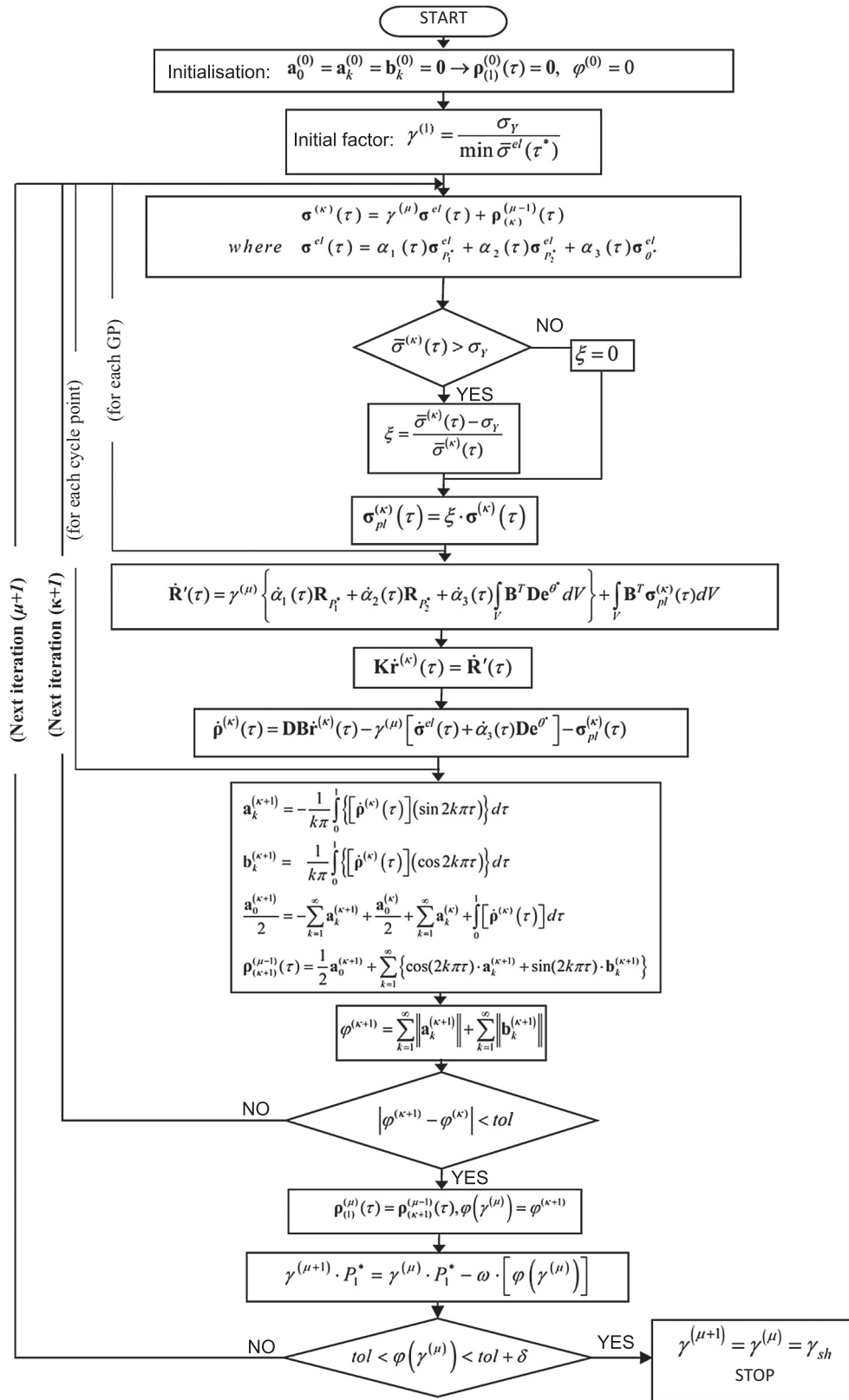


Fig. 3. Flow chart of the enhanced RSDM-S.

The equivalent stress $\bar{\sigma}^{(k)}$ is used to check whether the total stress (vector \vec{OC} in Fig. 4) exceeds the yield surface. Since no exact knowledge of the plastic strain rate $\dot{\epsilon}_{(k)}^{pl}$ (Fig. 4) is needed, the

amount of plastic straining is equivalenced [9] with the plastic stress vector $\sigma_{pl}^{(k)}$ which is part of the radial vector \vec{OC} and its magnitude is determined from the magnitude of \vec{OC} , proportionally

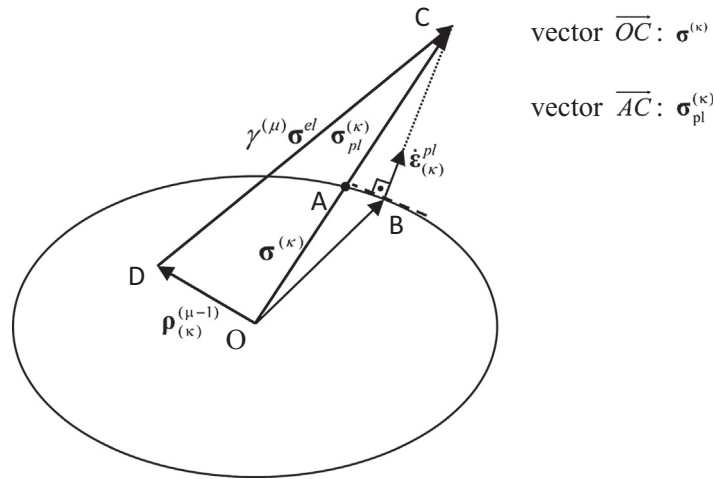


Fig. 4. Estimation of the plastic straining inside an iteration.

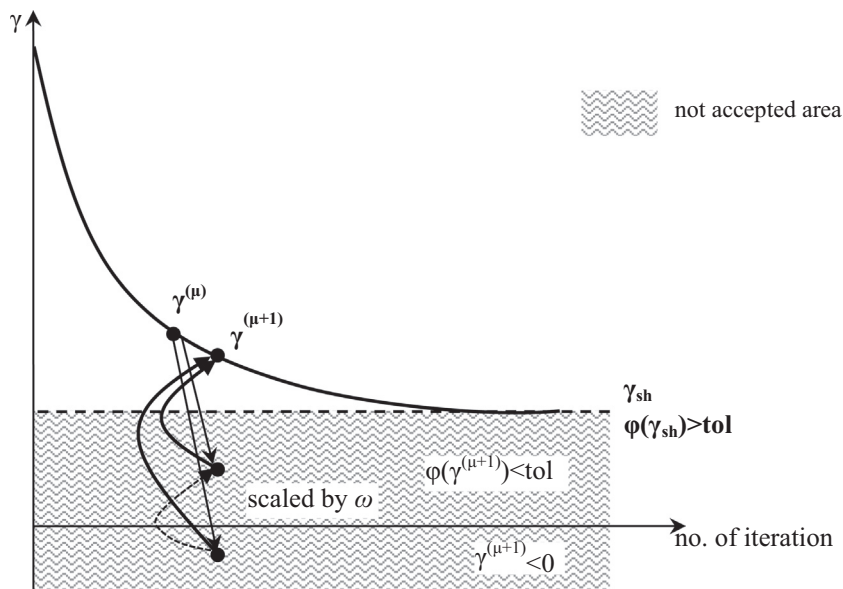


Fig. 5. Convergence scheme of the RSDM-S.

through the ratio ξ (Fig. 3). After applying this procedure to every Gauss point (GP) an equivalent plastic nodal vector is added to the nodal forces due to the mechanical and thermal loads to give $\mathbf{R}'(\tau)$ (whose expression may be seen in Fig. 3), which is then used to provide an estimate of the rate of the residual stresses $\dot{\mathbf{p}}(\tau)$ at the cycle point τ . Both these two expressions may be derived by combining Eqs. (16) and (3) and the fact that the residual stress rates are self-equilibrated (see, for example, [9,51]). Here again these two expressions would be augmented if more loads are applied.

The calculations are carried over for every cycle point and, by performing numerical time integration over all the cycle points, an update of the Fourier coefficients leading to an update of the residual stresses is obtained.

An update of the function φ which is the sum of the norms of the coefficients \mathbf{a}_k and \mathbf{b}_k in front of the trigonometric parts of the Fourier series is then calculated. This is checked against the previous iterate of φ and if it is found to be within a specified tolerance, we exit the inner loop [63]. The fact that two consecutive values of φ are virtually the same, leads to the conclusion that

$\mathbf{a}_k^{(k+1)} \rightarrow \mathbf{a}_k^{(k)}, \mathbf{b}_k^{(k+1)} \rightarrow \mathbf{b}_k^{(k)}$ which, in view of (14), guarantees that the residual stress rate solution has been stabilized, for the current loading factor. This is a new convergence criterion which, keeping the same accuracy, leads to a substantial reduction of the inner loop iterations as compared to the one adopted in the original publication [51] where the converged solution was judged on the updates of the full expressions of the residual stresses, including the constant terms.

The value of φ , being always positive, is then used to decrease the loading factor and thus perform the outer loop iterations which stop when the value of φ becomes virtually zero. This may be expressed through the following double inequality, which is also a different criterion to the one used in the original RSDM-S [51]:

$$tol < \varphi(\gamma^{(\mu)}) < tol + \delta \tag{19}$$

One obtains accurate results for a value of $tol \approx 10^{-3}$ with δ being an error tolerance, e.g. 10^{-4} .

A convergence parameter ω is needed (Fig. 3) so that the procedure always guarantees to converge. The numerical strategy is to

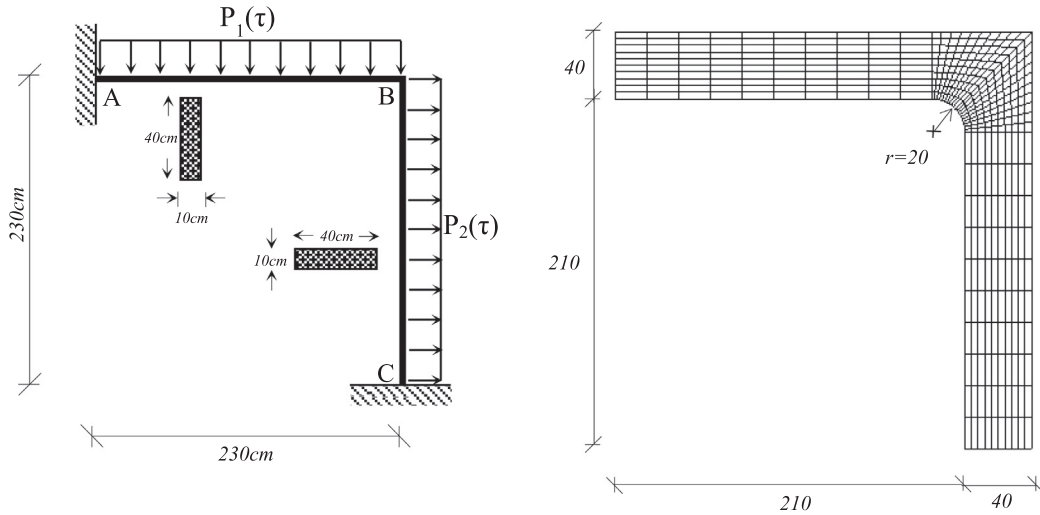


Fig. 6. Geometry, loading and finite element mesh of the frame.

Table 1
Material properties of the frame.

Young's modulus	E = 200 GPa
Poisson's ratio	ν = 0.3
Yield stress	σ _Y = 100 MPa

overshooting may result to even negative value of $\gamma^{(\mu+1)}$ (Fig. 5); the same strategy by halving ω is followed till we get a positive value of $\gamma^{(\mu+1)}$ which also satisfies $\varphi(\gamma^{(\mu+1)}) > tol$.

It should be noted here that when the conditions for shakedown have been reached, the plastic stress vector, as expected, also approaches zero, within some tolerance, at all the cycle points [51].

start the procedure with the convergence parameter $\omega = 1$. For many numerical examples, this normally leads to a monotonic convergence, from above, to the shakedown load.

It could happen however, especially when starting from a high initial value that an overshooting of the shakedown factor occurs. This means that the procedure bypasses the predefined tolerance tol for φ . To deal with the overshooting, a numerical convergence scheme is followed, which is depicted in Fig. 5. Thus, a loading factor $\gamma^{(\mu+1)}$ is evaluated at the current iteration $\mu + 1$ for which $\varphi(\gamma^{(\mu+1)}) < tol$; this cannot be accepted (inequality (19)) and the convergence factor is continuously halved until we get a loading factor for which $\varphi(\gamma^{(\mu+1)}) > tol$. In some other case an even bigger

4. 2-D loading domain examples

The numerical efficiency of the enhanced RSDM-S is demonstrated in a couple of examples consisted of a frame and a continuous beam subjected to two independent loads. Both the examples are modelled using quadrilateral continuum elements. Two different loading domains are considered that show the versatility of the approach.

4.1. Frame example

The first example is the frame of Fig. 6. The frame is assumed homogeneous, isotropic, elastic-perfectly plastic, having the material data shown in Table 1. The finite element mesh discretization

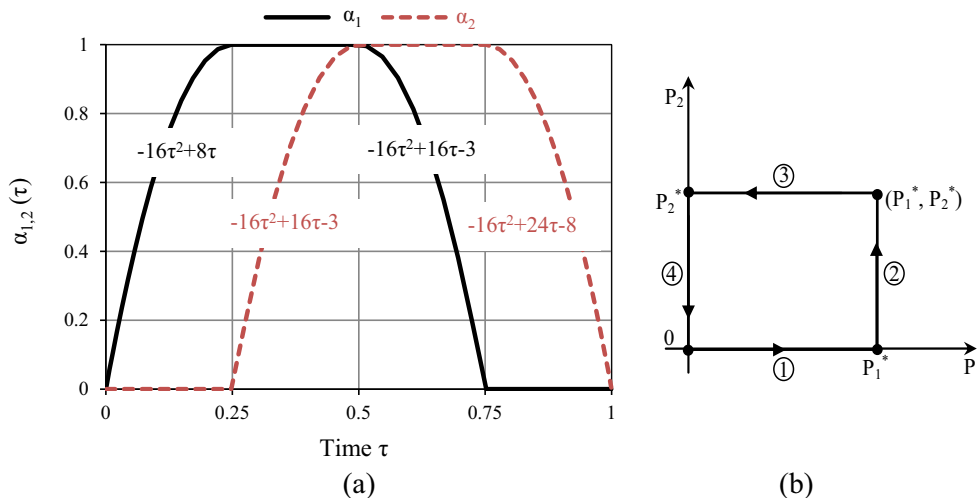


Fig. 7. Independent cyclic load variation over one time period in (a) time domain, (b) load domain.

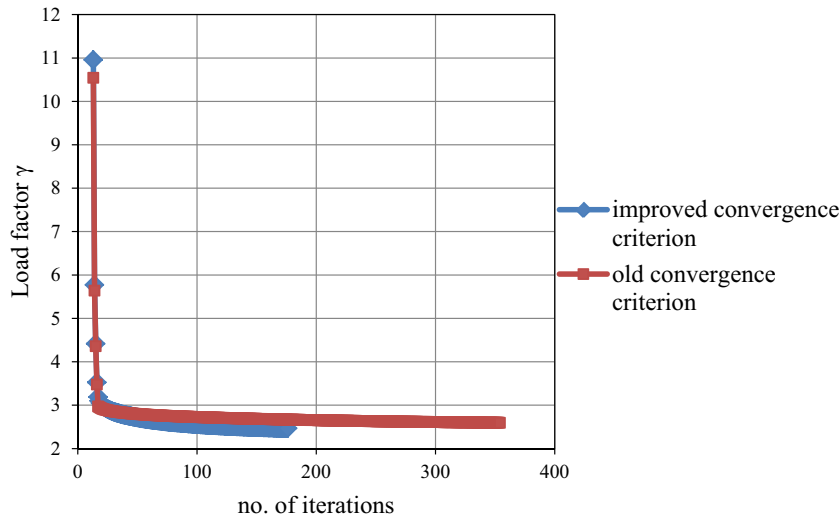


Fig. 8. Comparison of the two convergence criteria for the frame example.

of the frame, shown also in Fig. 6, consists of 400 eight-noded, iso-parametric elements with 3×3 Gauss integration points. The frame is subjected to two uniformly distributed loads $P_1(\tau)$ and $P_2(\tau)$, applied on the external faces of AB and BC, respectively.

4.1.1. Standard loading domain

A rectangular loading domain is considered with the two loads varying independently (Fig. 7), having maximum values $P_1^* = 3$ and $P_2^* = 1$, respectively, while their minimum values are equal to zero [51].

This example has been investigated in [39] using an edge-based smoothed finite element method (ES-FEM) and a primal-dual shakedown algorithm, and in [49] using a strain driven strategy. In those applications, however, the loading domains have one or both the minimum values different to zero unlike the loading domain used here, where the minimum values are both assumed zero. This more general kind of loading domain will be studied in the next section.

A prescribed loading in the time domain that passes through the four vertices of the rectangle, in a consecutive manner (Fig. 7 (b)), may be defined using the time functions $\alpha_1(\tau), \alpha_2(\tau)$ of Fig. 7 (a).

For this problem, the initial convergence parameter ω , in the process of the iterations, had to be halved twice, for the procedure to converge to the final shakedown factor which was found equal to 2.47.

A number of 175 iterations were required to converge. The amount of CPU time needed to solve this problem, for an Intel Core i7 at 2.93 GHz with 4096 MB RAM, was around 160 s.

On the other hand, using the old convergence criterion, convergence was achieved after 280 s (CPU time), with 354 iterations [51]. Thus, it is realized that using the proposed enhanced procedure there is a significant acceleration (about 43%).

The convergence of the two procedures, the old and the new one, may be seen in Fig. 8. For better illustration reasons, the common 10 first iterations are not plotted.

4.1.2. Loading domain with different than zero origin

A rectangular loading domain is considered herein with the two loads $P_1(\tau)$ and $P_2(\tau)$ varying independently, between the values [1.2, 3] and [0.4, 1] respectively (Fig. 9).

A prescribed loading in time domain that passes through the four vertices of the rectangle, in a consecutive manner, may be defined using the following equations:

$$P(\tau) = \begin{Bmatrix} P_1(\tau) \\ P_2(\tau) \end{Bmatrix} = \begin{Bmatrix} P_1^* \alpha_1(\tau) \\ P_2^* \alpha_2(\tau) \end{Bmatrix} \quad \text{where the time functions } \alpha_1(\tau), \alpha_2(\tau) \text{ are :}$$

$$\begin{aligned} \alpha_1(\tau) &= -9.6\tau^2 + 4.8\tau + 0.4, & \alpha_2(\tau) &= 0.4, & \tau &\in [0, 1/4] \\ \alpha_1(\tau) &= 1, & \alpha_2(\tau) &= -9.6\tau^2 + 9.6\tau - 1.4, & \tau &\in (1/4, 1/2] \\ \alpha_1(\tau) &= -9.6\tau^2 + 9.6\tau - 1.4, & \alpha_2(\tau) &= 1, & \tau &\in (1/2, 3/4] \\ \alpha_1(\tau) &= 0.4, & \alpha_2(\tau) &= -9.6\tau^2 + 14.4\tau - 4.4, & \tau &\in (3/4, 1] \end{aligned} \quad (20)$$

In this case $P_1^* = 3, P_2^* = 1$ and $0.4 \leq \alpha_1(\tau), \alpha_2(\tau) \leq 1$ (see Fig. 10).

For this example, the initial convergence parameter ω , in the process of the iterations, had to be halved twice, for the RSDM-S to converge to the final shakedown limit which was found equal to 3.91.

The comparison between the enhanced RSDM-S solution and those of different analysis methods in the literature, are shown in Table 2. It may be seen that they match quite well.

4.2. Symmetric continuous beam under distributed load

A symmetric three-span continuous beam under uniform loads is considered next. Due to symmetry, only half of the beam is ana-

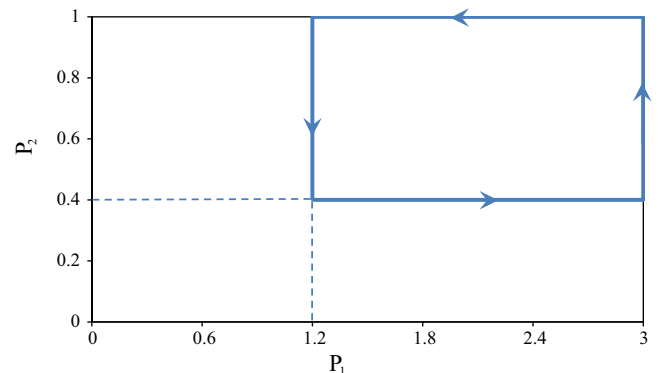


Fig. 9. Loading domain of the frame example.

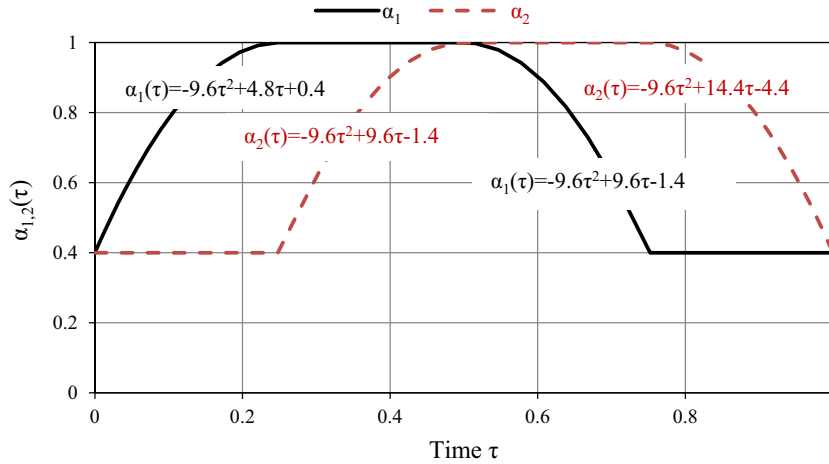


Fig. 10. Time functions variation, over one period corresponding to the load domain of Fig. 9.

Table 2 Comparison of numerical results of the frame.

Author	Shakedown factor
Garcea et al. [48]	3.925
Tran et al. [39]	4.006
Pham [64]	4.015
Present	3.91

Table 3 Material properties of the symmetric continuous beam example.

Young's modulus	E = 180 GPa
Poisson's ratio	ν = 0.3
Yield stress	σ _Y = 100 MPa

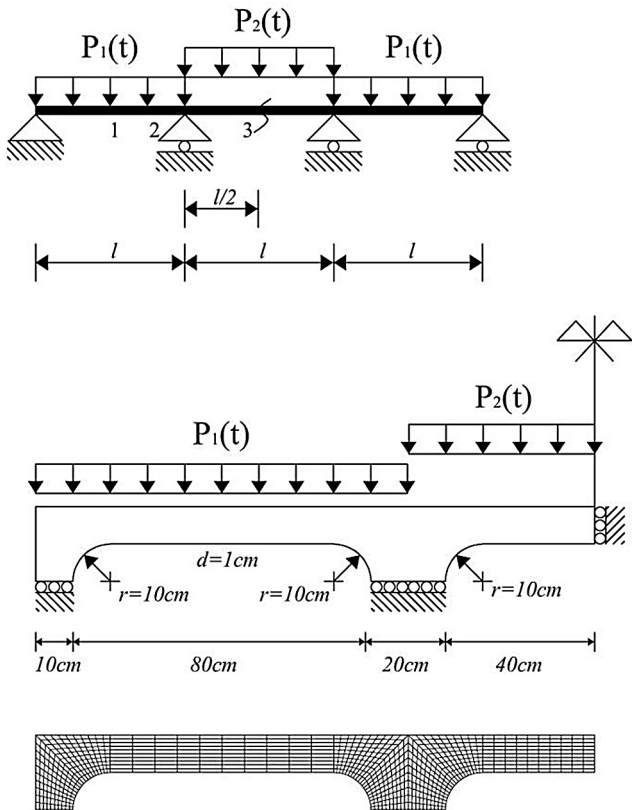


Fig. 11. Geometry, loading and finite element mesh of the continuous beam.

lyzed (Fig. 11). This is a relatively large scale problem since its finite element discretization consists of 800 eight-noded, isoparametric elements with 3 × 3 Gauss integration points (Fig. 11).

The beam is assumed homogeneous, isotropic, elastic-perfectly plastic, having the material data of Table 3.

4.2.1. Standard loading domain

The rectangular loading domain of Fig. 7 was considered first. The loads vary in the domain $P_1 \in [0, P_1^*]$ and $P_2 \in [0, P_2^*]$ where $P_1^* = 1$ and $P_2^* = 2$ [51].

This example has also been treated in [48,64] using a different loading domain, that has its origin different to zero, to the one employed here. This particular load domain will be studied in the next section.

A prescribed loading in the time domain that passes through the four vertices of the rectangle, may be defined by using the same time functions $\alpha_1(\tau), \alpha_2(\tau)$ of Fig. 7.

For this example, the initial convergence parameter ω , in the process of the iterations, had to be halved three times, for the procedure to converge to the final shakedown factor which was found equal to 0.191. Once again although the starting point was quite high as compared to the final result, the initial descent was rapid in just 12 iterations, as shown in Fig. 12.

The convergence of the enhanced RSDM-S, based on the new criterion, and its comparison with the old one, may be seen in Fig. 12. For a better illustration of the comparison, the first 10 iterations are not plotted.

A number of 65 iterations were required to converge, whereas 100 iterations were needed with the old criterion [51]. The amount of CPU time needed to solve this problem was around 220 s which is around 40% faster.

4.2.2. Loading domain with different than zero origin

A rectangular loading domain is considered (Fig. 13) with the two loads varying independently, as $P_1 \in [1.2, 2], P_2 \in [0, 1]$.

A prescribed loading in the time domain that passes through the four vertices of the rectangle, in a consecutive manner, may be defined by using the following time functions $\alpha_1(\tau), \alpha_2(\tau)$ (Fig. 14):

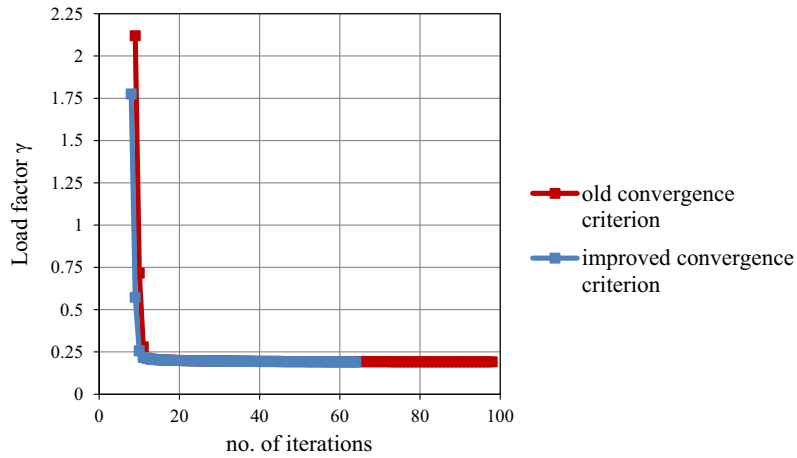


Fig. 12. Comparison of the two convergence criteria for the beam example.

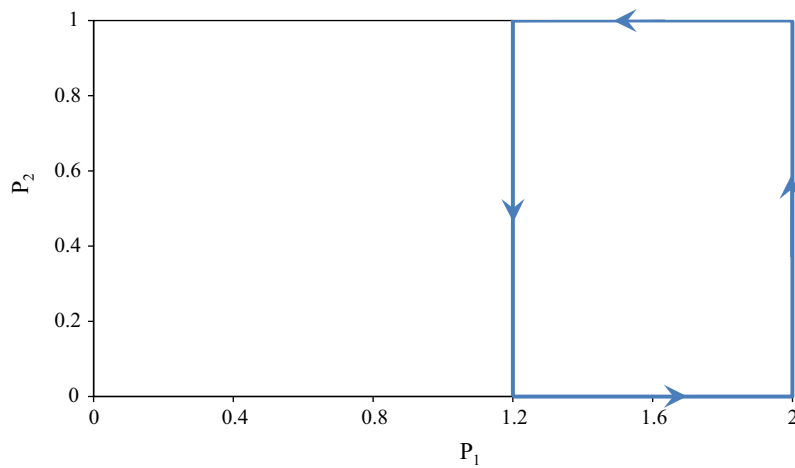


Fig. 13. Loading domain of the beam example.

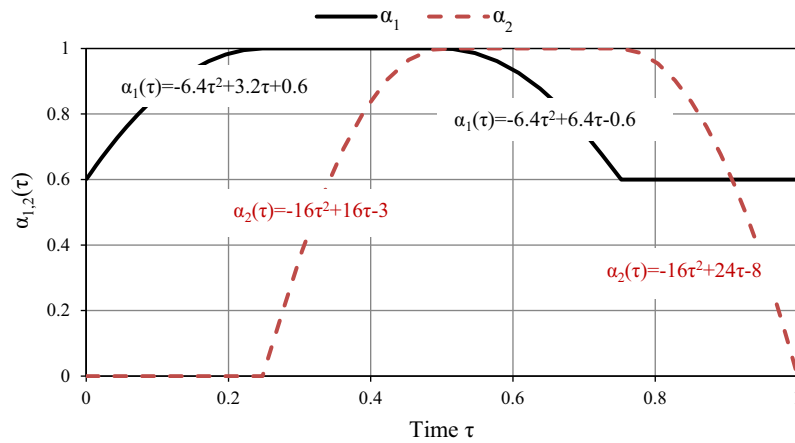


Fig. 14. Time functions variation, over one period corresponding to the load domain of Fig. 13.

$$\begin{aligned}
 \alpha_1(\tau) &= -6.4\tau^2 + 3.2\tau + 0.6, & \alpha_2(\tau) &= 0, & \tau &\in [0, 1/4] \\
 \alpha_1(\tau) &= 1, & \alpha_2(\tau) &= -16\tau^2 + 16\tau - 3, & \tau &\in (1/4, 1/2] \\
 \alpha_1(\tau) &= -6.4\tau^2 + 6.4\tau - 0.6, & \alpha_2(\tau) &= 1, & \tau &\in (1/2, 3/4] \\
 \alpha_1(\tau) &= 0.6, & \alpha_2(\tau) &= -16\tau^2 + 24\tau - 8, & \tau &\in (3/4, 1]
 \end{aligned}
 \tag{21}$$

In this case $P_1^* = 2$, $P_2^* = 1$ and $0.6 \leq \alpha_1(\tau) \leq 1, 0 \leq \alpha_2(\tau) \leq 1$ (Fig. 14).

For this example, the initial convergence parameter ω , in the process of the iterations, had to be halved three times, for the RSDM-S to converge to the final shakedown limit which was found

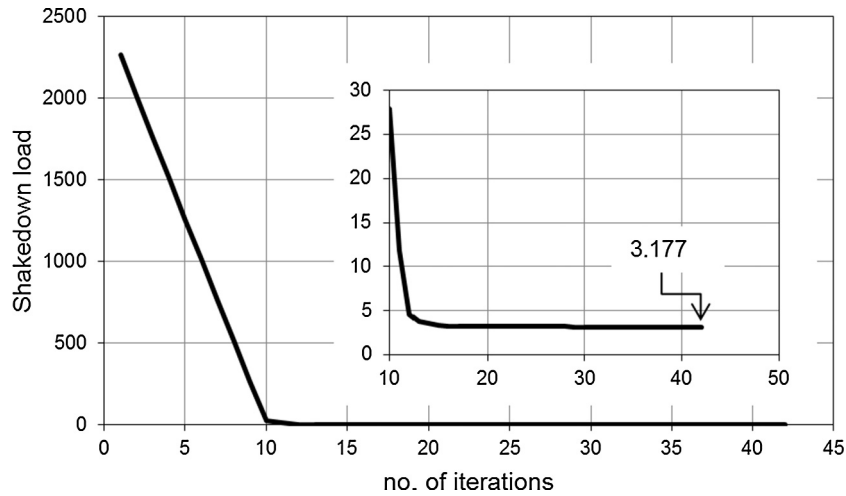


Fig. 15. Convergence of the RSDM-S towards the shakedown factor for the continuous beam problem.

Table 4
Comparison of numerical results of the symmetric continuous beam.

Author	Shakedown limit
Garcea et al. [48]	3.244
Tran et al. [39]	3.377
Pham [64]	3.264
Present	3.177

Table 5
Material properties of the plate.

Young's modulus	$E = 208 \text{ GPa}$
Poisson's ratio	$\nu = 0.3$
Yield stress	$\sigma_Y = 360 \text{ MPa}$
Coefficient of thermal expansion	$5 \times 10^{-5} \text{ }^\circ\text{C}^{-1}$

equal to 3.177. Less than 50 iterations were required for this problem to converge (Fig. 15). In the insert of the figure, one may see, after the initial descent, the last iterates towards the shakedown value.

The shakedown factor obtained by the enhanced RSDM-S, and its comparison with the results of different analysis methods, is shown in Table 4. It may be seen that there is a good agreement.

5. 3-D loading domain example

Let us consider the holed square plate of Fig. 16 subjected to a three-dimensional loading consisting of a thermal load, i.e. a temperature difference $\Delta\theta(\tau)$ between the edge of the hole and the edge of the plate, and two uniformly distributed mechanical loads $P_1(\tau)$ and $P_2(\tau)$. The plate is assumed homogeneous, isotropic, elastic-perfectly plastic with the material data of Table 5.

Concerning the geometrical characteristics of the plate, the ratio between the diameter D of the hole and the length L of the plate is equal to 0.2 and the ratio of the thickness d of the plate to its length is equal to 0.05. For this study $L = 20 \text{ cm}$ has been chosen.

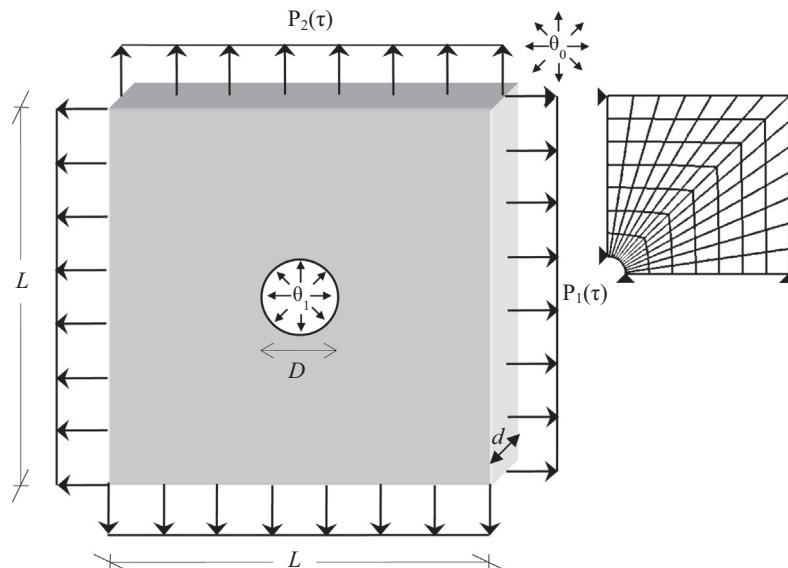


Fig. 16. Geometry, and finite element discretization of the plate subjected to mechanical and thermal loading.

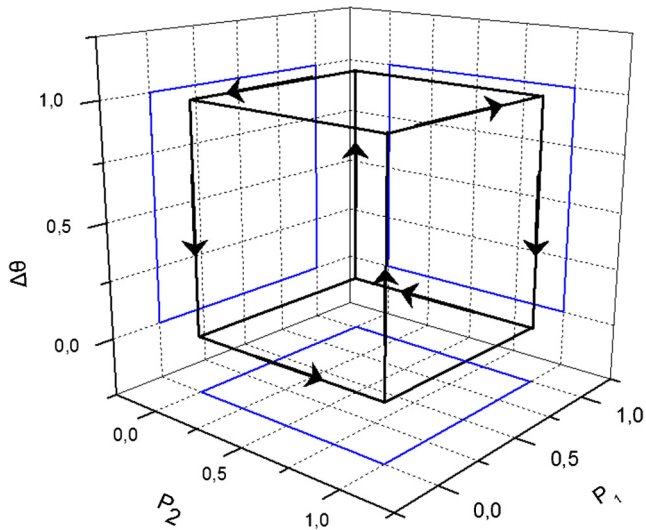


Fig. 17. Three - dimensional load domain.

Table 6
Numerical results of shakedown analysis in three-dimensional loading space.

$(P_1^*, P_2^*, \Delta\theta^*)$	P_1/σ_Y	P_2/σ_Y	$\sigma_t/2\sigma_Y$
(1,0,0)	0.7	0	0
(0,1,0)	0	0.7	0
(0,0,1)	0	0	1.002
(1,1,0)	0.522	0.522	0
(1,0,1)	0.566	0	0.196
(1,1,1)	0.448	0.448	0.156
(1,0.5,1)	0.507	0.254	0.176
(1,0.5,0.5)	0.547	0.274	0.048
(1,1,0.5)	0.484	0.484	0.042
(0.5,0.5,1)	0.388	0.388	0.269
(0.5,1,0.5)	0.275	0.549	0.048

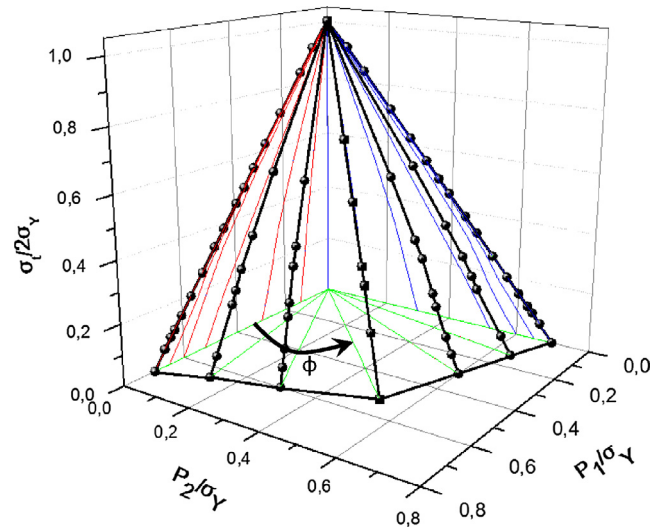


Fig. 19. Shakedown domain in three-dimensional loading space.

Due to the symmetry of the structure and the loading, only one quarter of the plate is analyzed. The finite element mesh discretization of the plate is also shown in Fig. 16. Ninety-eight, eight-noded, iso-parametric elements with 3×3 Gauss integration points were used.

The variation of the temperature with radius r has the same logarithmic distribution as in [52]:

$$\theta(r, \tau) = \theta_0 + \frac{\Delta\theta(\tau) * \ln\left(\frac{5D/2}{r}\right)}{\ln 5} \quad (22)$$

The above relation describes the temperature variation inside the plate giving a value of $\theta_1(\tau) = \theta_0 + \Delta\theta(\tau)$ around the edge of the hole ($r = D/2$) and $\theta_1 = \theta_0$ at the outer edges of the plate ($r = 5D/2$). The temperature θ_0 is assumed to be equal to zero. It should be noted that, in the results, σ_t denotes the maximum effective thermal elastic stress due to the fluctuating temperature.

The loads vary independently in the three-dimensional loading domain of Fig. 17 having the following variations:

$$P_1 \in [0, P_1^*], \quad P_2 \in [0, P_2^*], \quad \Delta\theta \in [0, \Delta\theta^*]$$

where the maximum values are $P_1^* = P_2^* = \Delta\theta^*$.

In the same figure one can see, starting from the origin, the successive movement that passes through the eight vertices of the loading domain that may define a prescribed loading. This loading may be realized in the time domain by the following expression:

$$P(\tau) = \begin{Bmatrix} P_1^* \alpha_1(\tau) \\ P_2^* \alpha_2(\tau) \\ \Delta\theta^* \alpha_3(\tau) \end{Bmatrix}, \quad \text{where the time functions}$$

$\alpha_1(\tau), \alpha_2(\tau), \alpha_3(\tau)$ are (Fig. 18):

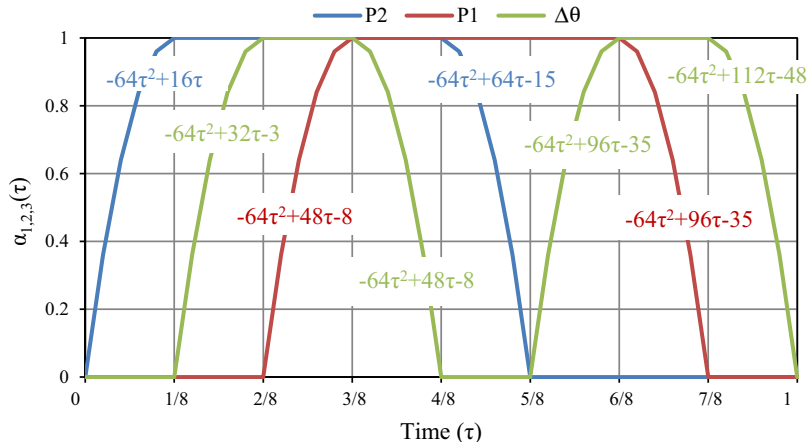


Fig. 18. Time functions variation, over one period corresponding to the three-dimensional load domain of Fig. 17.

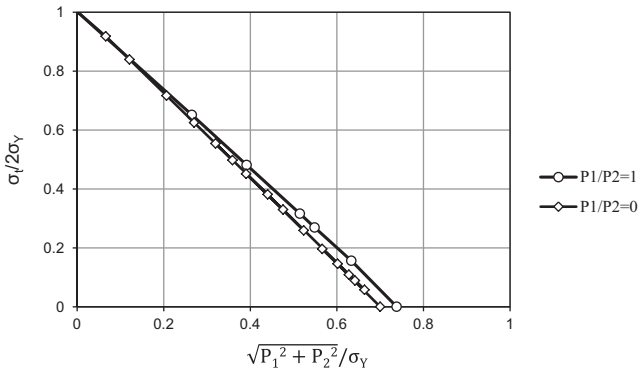


Fig. 20. Shakedown domains in planes for fixed ratios (P_1^*/P_2^*).

$$\begin{aligned}
 &\alpha_1(\tau) = 0, \quad \alpha_2(\tau) = -64\tau^2 + 16\tau, \quad \alpha_3(\tau) = 0, \quad \tau \in [0, 1/8] \\
 &\alpha_1(\tau) = 0, \quad \alpha_2(\tau) = 1, \quad \alpha_3(\tau) = -64\tau^2 + 32\tau - 3, \quad \tau \in (1/8, 2/8] \\
 &\alpha_1(\tau) = -64\tau^2 + 48\tau - 8, \quad \alpha_2(\tau) = 1, \quad \alpha_3(\tau) = 1, \quad \tau \in (2/8, 3/8] \\
 &\alpha_1(\tau) = 1, \quad \alpha_2(\tau) = 1, \quad \alpha_3(\tau) = -64\tau^2 + 48\tau - 8, \quad \tau \in (3/8, 4/8] \\
 &\alpha_1(\tau) = 1, \quad \alpha_2(\tau) = -64\tau^2 + 64\tau - 15, \quad \alpha_3(\tau) = 0, \quad \tau \in (4/8, 5/8] \\
 &\alpha_1(\tau) = 1, \quad \alpha_2(\tau) = 0, \quad \alpha_3(\tau) = -64\tau^2 + 96\tau - 35, \quad \tau \in (5/8, 6/8] \\
 &\alpha_1(\tau) = -64\tau^2 + 96\tau - 35, \quad \alpha_2(\tau) = 0, \quad \alpha_3(\tau) = 1, \quad \tau \in (6/8, 7/8] \\
 &\alpha_1(\tau) = 0, \quad \alpha_2(\tau) = 0, \quad \alpha_3(\tau) = -64\tau^2 + 112\tau - 48, \quad \tau \in (7/8, 1]
 \end{aligned} \tag{23}$$

In Table 6 one may see the resulted shakedown factor for some specific ratios of $P_1^*/P_2^*/\Delta\theta^*$.

Finally, the 3D shakedown domain of the problem is shown in Fig. 19. It should be mentioned that each solution for different fixed ratios P_1^*/P_2^* , represents a fixed angle φ in the $P_1 - P_2$ -plane. Thus, the results may be presented as a sequence of two dimensional plots. In Figs. 20, 21, two-dimensional plots of the results obtained by RSDM-S, for different fixed ratios P_1^*/P_2^* , are presented.

Plotting the results in the three planes, the horizontal plane (Fig. 22) or either of the two (due to the symmetry) vertical ones (Fig. 23), one may see the results of the RSDM-S for a two-dimensional loading case consisted of a mechanical and a thermal or of two mechanical loads. These results are in perfect agreement with the results of the method that was formulated for 2-dimensional loading [52].

The CPU time needed for the RSDM-S to converge, for a typical case of $P_1^* = P_2^* = \Delta\theta^*$, was about 50 s on the same, as above, processor. A total number of 40 time points proved enough to describe

the total 3D loading domain. In Fig. 24 one may see a typical convergence behavior of the RSDM-S i.e. for the fixed ratios $P_1^*/P_2^*/\Delta\theta^* = 1$. The initial value of $\omega = 1$ was sufficient for convergence.

An important observation is that both the CPU time and the iterations needed for the RSDM-S to converge in the case of 3D loading domain, are of the same order with the ones required for the case of the 2D loading domain [52]. On the contrary, for the problem solved through the use of an IPM algorithm, there is a significant increase of the running time between the two cases, since the number of variables and the number of constraints, in the three-dimensional loading case are virtually twice the number in the two-dimensional case [55].

6. Generalization for n-dimensional loading domain

As it may also be seen by the proof in Section 2, the theorem of König and Kleiber [60] is not associated with any specific form of a cyclic loading. Thus, one may use any prescribed cyclic loading, which passes through the vertices that define the loading domain, as long as it is on or within the boundaries of this domain. One would expect, of course, a non-uniqueness of the residual stresses of the limit cycle for the different prescribed loadings.

The cyclic loading used so far, follows the boundaries of the domain and it may be automated for 2D and 3D loading domains. In cases, however, of more than three independent loads, this automation becomes more difficult.

We enter the discussion towards this automation, by considering an alternative cyclic loading program for a 2D loading domain, which may be seen in Fig. 25(a). This loading comprises of a movement going from the origin to each vertex and coming back, before moving to the next vertex. The time functions that may describe such movement, inside a period, can simply be sine functions (Fig. 25(b)). For $\tau_1 = \tau_2 = \tau_3 = 1/3$, these functions may be written as:

$$\alpha(\tau) = \begin{cases} \sin(3\pi\tau), & \tau \in [0, 1/3] \\ \sin(3\pi\tau - \pi), & \tau \in (1/3, 2/3] \\ \sin(3\pi\tau - 2\pi), & \tau \in (2/3, 1] \end{cases} \tag{24}$$

To reach all the three vertices of the loading domain, each of these time functions are multiplied by either P_1^* or P_2^* , separately, or simultaneously (Fig. 25(b)).

Equivalently moving from the origin and back to each of the seven vertices in a 3D loading domain (Fig. 26(a)), an alternative cyclic loading program to the one proposed previously, may be

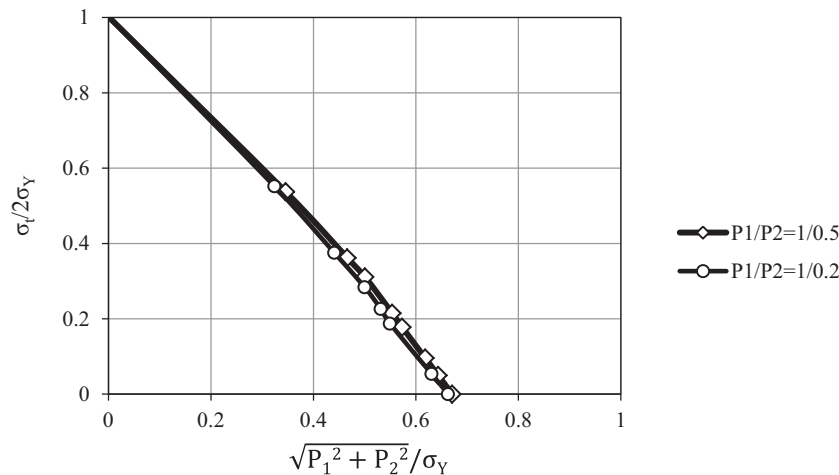


Fig. 21. Shakedown domains in planes for fixed ratios (P_1^*/P_2^*).

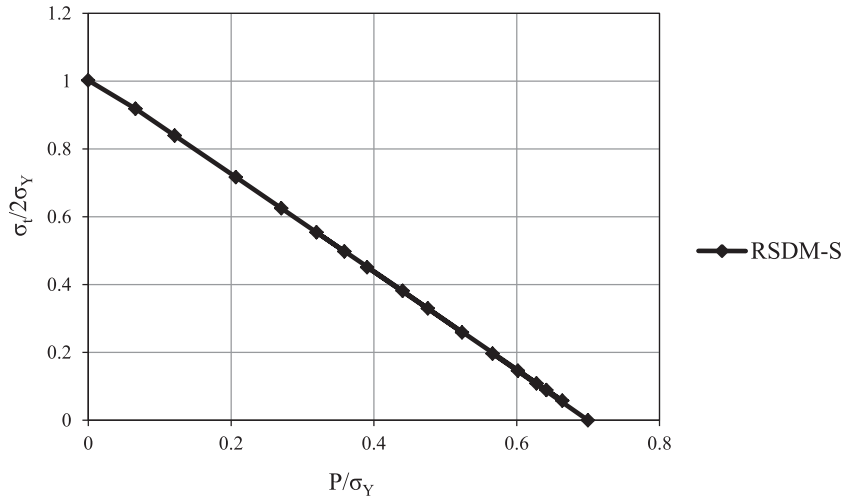


Fig. 22. Shakedown domain produced by the RSDM-S for a two dimensional loading case (independent variation of thermal and mechanical load, rectangular loading domain) [52].

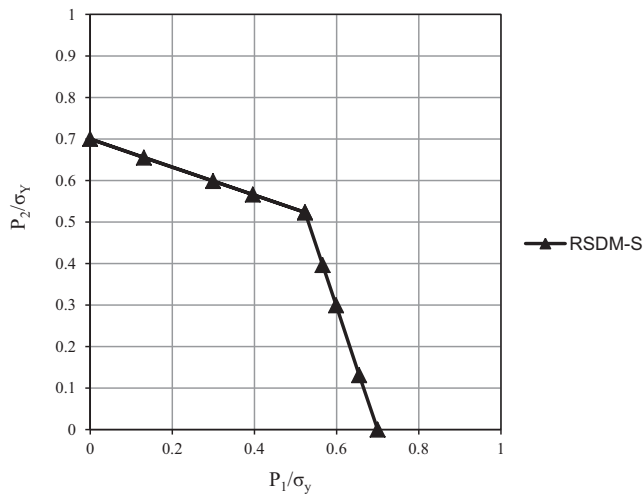


Fig. 23. Shakedown domain produced by RSDM-S for a two-dimensional loading case (without temperature, rectangular loading domain) [51].

seen in Fig. 26(b). The sine time functions that divide, equally and consecutively a period, in this case, take the form:

$$\alpha(\tau) = \begin{cases} \sin(7\pi\tau), & \tau \in [0, 1/7] \\ \sin(7\pi\tau - \pi), & \tau \in (1/7, 2/7] \\ \sin(7\pi\tau - 2\pi), & \tau \in (2/7, 3/7] \\ \sin(7\pi\tau - 3\pi), & \tau \in (3/7, 4/7] \\ \sin(7\pi\tau - 4\pi), & \tau \in (4/7, 5/7] \\ \sin(7\pi\tau - 5\pi), & \tau \in (5/7, 6/7] \\ \sin(7\pi\tau - 6\pi), & \tau \in (6/7, 1] \end{cases} \quad (25)$$

In order to reach the seven vertices of the 3D loading domain, we may see from Fig. 26(b) that the first three time functions are multiplied by the maximum values of the three loads, the next three by their combination under pairs and the last one by all three of them.

The use of the sine functions for both the 2D and 3D loading domain contributes, obviously, towards the automation of the loading program. The above alternative loadings paths are applied for the example of the holed squared plate of Fig. 16. A 2D loading case for $P_1^* = P_2^*$ (Fig. 23), and a 3D loading case for $P_1^* = P_2^* = \Delta\theta^*$, obtained, using the same number of time points, virtually the same

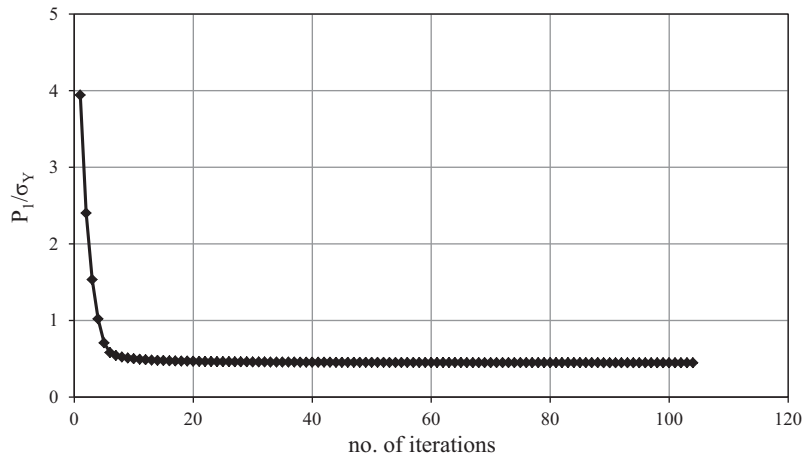


Fig. 24. Convergence of the RSDM-S towards the shakedown factor for the three-dimensional loading case.

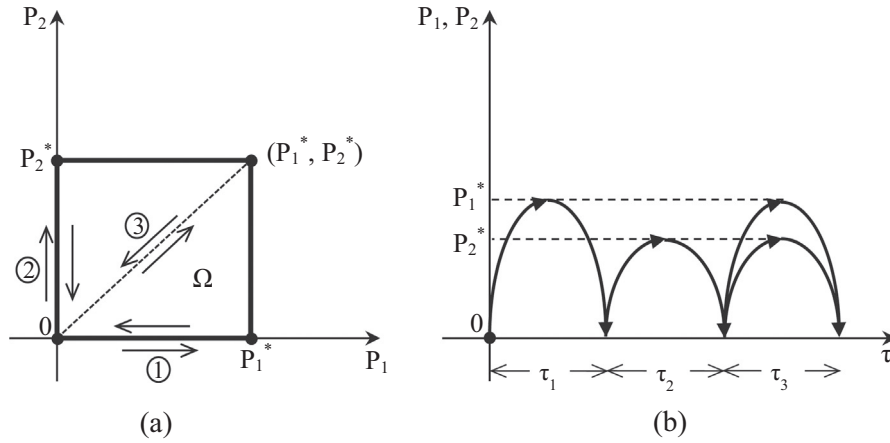


Fig. 25. Alternative cyclic loading program for the 2D case.

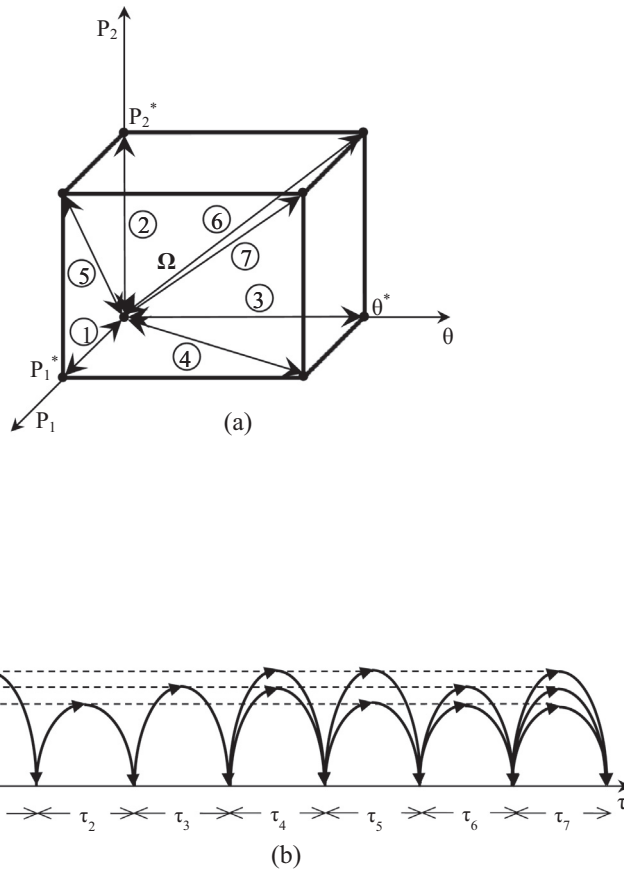


Fig. 26. Alternative cyclic loading program for the 3D case.

shakedown load of $0.52\sigma_y$ and $0.45\sigma_y$ respectively, that was obtained with the original load paths of Figs. 7 and 17. For the 3D case, in particular, one may see the convergence behavior of the two different loading paths, using the same number of 40 time points, in Fig. 27. As it may be seen, the penalty to pay towards the automation of the loading program is that the alternative load path requires a relatively bigger amount of iterations to converge to the shakedown load.

The discussion above paves the way to generalize for any number of loads. Thus, for an n -dimensional loading domain, defined by

its origin and $m = 2^n - 1$ vertices, one may write the m sine time functions for the equal splitting of the period:

$$\alpha_l(\tau) = \sin(m\pi\tau - (l-1)\pi), \quad \frac{l-1}{m} \leq \tau \leq \frac{l}{m}, \quad l = 1, \dots, m \quad (26)$$

Since each vertex of the n -cuboid, except for the origin, corresponds to a combination of the maximum values of each load, it may be seen from (11) that the first $\binom{n}{1}$ time functions should be multiplied by each of these values, the next $\binom{n}{2}$ time functions

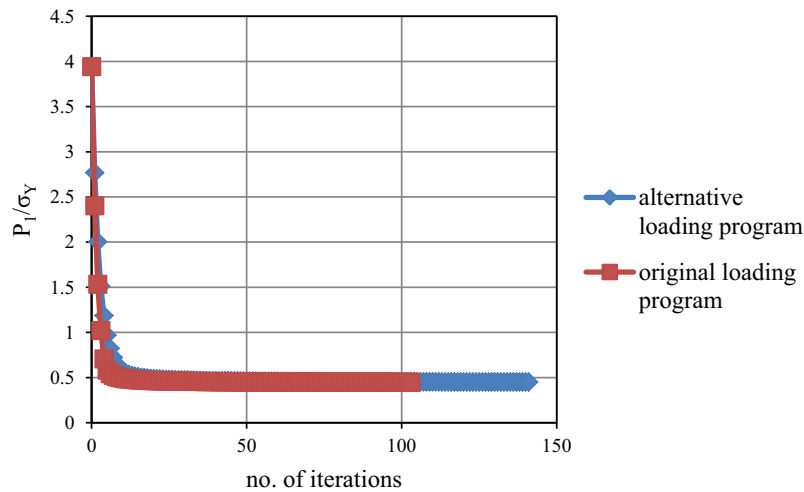


Fig. 27. Convergence for the two different cyclic loading programs (3D case).

by their combination every two, the next $\binom{n}{3}$ by their combination every three, and so on. These combinations may be retrieved using any combinatorial algorithm (e.g. [65]). Thus, the whole procedure in any n -dimensional loading space may be fully automated. This effective and robust formulation is of particular importance since, when designing structures, there will be cases where the number of independent loads would be much higher than three (e.g. [66,67]). It should also be underlined that the procedure may be embedded in any existing FE code.

7. Conclusions

An efficient novel iterative numerical procedure, called RSDM-S, for the shakedown analysis of elastoplastic structures loaded by independently varying cyclic loads, was presented. The method is improved and enhanced over the original approach that appeared recently in the literature and concerned a 2D loading domain. The following improvements and enhancements have been presented herein:

- Both approaches, in the course of iterations use two iteration loops, one inside the other. In the present approach, a new convergence criterion is proposed which reduces the inner loop iterations with an effect to make the current version twice as fast.
- The present approach is formulated in a 3D thermomechanical loading domain, using time functions that follow the outline of this domain. It has to be noted that very few shakedown results exist in the literature, for such a domain, although it may often occur in practice. Extending the dimensions of the loading domain from 2D to 3D hardly increases the computational time, which is not the case with any procedure that uses a MP algorithm, where the computational time more than doubles.
- Next, a generalization of the procedure is proposed, so that it applies to any multiple loading domain. As a result of this domain, a convex hull that consists of vertices that mark all the possible combinations of the load peaks may be visualized. A cyclic loading program which visits each vertex and comes back to the origin is suggested. The use of sine-type time functions that split the period of the cyclic loading, combined with a combinatorial algorithm represent these visits effectively and automate the procedure. The approach appears also very effi-

cient with many loads, since, irrespective of their number, the loads participate just through their corresponding elastic stresses, which are calculated, once and for all, at the beginning of the algorithm.

References

- [1] Drucker DC. A definition of stable material. *ASME J Appl Mech* 1959;26:101–6.
- [2] Zarka J, Engel JJ, Inglebert G. On a simplified inelastic analysis of structures. *Nucl Eng Des* 1980;57:333–68.
- [3] Zarka J. Direct analysis of elastic–plastic structures with overlay materials during cyclic loading. *Int J Numer Meth Eng* 1980;15:225–35.
- [4] Hübel H. Simplified theory of plastic zones for cyclic loading and multilinear hardening. *Int J Press Vess Pip* 2015;129:19–31.
- [5] Ponter ARS, Carter KF. Shakedown state simulation techniques based on linear elastic solutions. *Comput Methods Appl Mech Eng* 1997;140:259–79.
- [6] Ponter ARS, Chen HF. A minimum theorem for cyclic loading in excess of shakedown, with applications to the evaluation of a ratchet limit. *Eur J Mech A/Solids* 2001;20:539–54.
- [7] Maitournam MH, Pommier B, Thomas JJ. Détermination de la réponse asymptotique d'une structure anélastique sous chargement thermomécanique cyclique. *CR Mec* 2002;330:703–8.
- [8] Zouain N, Sant'Anna R. Computational formulation for the asymptotic response of elastoplastic solids under cyclic loads. *Eur J Mech A/Solids* 2017;61:267–78.
- [9] Spiliopoulos KV, Panagiotou KD. A direct method to predict cyclic steady states of elastoplastic structures. *Comput Methods Appl Mech Eng* 2012;223:186–98.
- [10] Spiliopoulos KV, Panagiotou KD. The residual stress decomposition method (RSDM): a novel direct method to predict cyclic elastoplastic states. In: Spiliopoulos K, Weichert D, editors. *Direct methods for limit states in structures and materials*. Dordrecht: Springer Science + Business Media; 2014. p. 139–55.
- [11] Melan E. Zur Plastizität des räumlichen Kontinuums. *Ing Arch* 1938;9:116–26.
- [12] Koiter WT. General theorems for elastic–plastic structures. In: Sneddon IN, Hill R, editors. *Progress in solid mechanics*. Amsterdam: North-Holland Publ Co; 1960. p. 165–221.
- [13] Prager W. Shakedown in elastic–plastic media subjected to cycles of load and temperature. In: *Proc Symp Plasticita nella Scienza delle Costruzioni*, Bologna. p. 239–44.
- [14] de Donato O. Second shakedown theorem allowing for cycles of both loads and temperature. *1st Lomb Sci Lett (A)* 1970;104:265–77.
- [15] Weichert D. On the influence of geometrical nonlinearities on the shakedown of elastic–plastic structures. *Int J Plast* 1986;2:135–48.
- [16] Gross-Weege J. A unified formulation of statical shakedown criteria for geometrically nonlinear problems. *Int J Plast* 1990;6:433–47.
- [17] Belouchrani MA, Weichert D. An extension of the static shakedown theorem to inelastic cracked structures. *Int J Mech Sci* 1999;41:163–77.
- [18] Pham D. Shakedown theory for elastic plastic kinematic hardening bodies. *Int J Plast* 2007;23:1240–59.
- [19] Stein E, Zhang G, König JA. Shakedown with nonlinear strain-hardening including structural computation using finite element method. *Int J Plast* 1992;8:1–31.
- [20] Simon JW. Direct evaluation of the limit states of engineering structures exhibiting limited, nonlinear kinematical hardening. *Int J Plast* 2013;42:141–67.

- [21] Bouby C, Kondo D, de Saxcé G. A comparative analysis of two formulations for nonlinear hardening plasticity models: application to shakedown analysis. *Eur J Mech A/Solids* 2015;53:48–61.
- [22] Pycko S, Maier G. Shakedown theorems for some classes of non-associative hardening elastic–plastic material models. *Int J Plast* 1995;11:367–95.
- [23] Bousshine L, Chaaba A, de Saxcé G. A new approach to shakedown analysis for non-standard elastoplastic material by the bipotential. *Int J Plast* 2003;19:583–98.
- [24] Polizzotto C. Shakedown theorems for elastic–plastic solids in the framework of gradient plasticity. *Int J Plast* 2008;24:218–41.
- [25] Polizzotto C. Shakedown analysis within the framework of strain gradient plasticity. In: Fuschi P, Pisano AA, Weichert D, editors. *Direct methods for limit and shakedown analysis of structures*. Switzerland: Springer International Publishing; 2015. p. 221–52.
- [26] Maier G. Shakedown theory in perfect elastoplasticity with associated and nonassociated flow-laws: a finite element, linear programming approach. *Meccanica* 1969;4:1–11.
- [27] Cohn MZ, Maier G. *Engineering plasticity by mathematical programming*. In: *Proceedings of NATO advanced study institute*. New York: Pergamon Press; 1977.
- [28] Zhang T, Raad L. An eigen-mode method in kinematic shakedown analysis. *Int J Plast* 2002;18:71–90.
- [29] Ngo NS, Tin-Loi F. Shakedown analysis using the p-adaptive finite element method and linear programming. *Eng Struct* 2007;29:46–56.
- [30] Arditto R, Cocchetti G, Maier G. On structural safety assessment by load factor maximization in piecewise linear plasticity. *Eur J Mech A/Solids* 2008;27:859–81.
- [31] Heitzer M, Pop G, Staat M. Basis reduction for the shakedown problem for bounded kinematic hardening material. *J Glob Opt* 2000;17:185–200.
- [32] Zouain N, Borges L, Silveira JL. An algorithm for shakedown analysis with nonlinear yield function. *Comput Methods Appl Mech Eng* 2002;191:2463–81.
- [33] Andersen KD, Christiansen E, Cohn AR, Overton ML. An efficient primal–dual interior point method for minimizing a sum of Euclidian norms. *SIAM J Sci Comput* 2000;22:243–62.
- [34] Vu DK, Yan AM, Nguyen-Dang H. A primal–dual algorithm for shakedown analysis of structures. *Comput Methods Appl Mech Eng* 2004;193:4663–74.
- [35] Magoarić H, Bourgeois S, Débordes O. Elastic plastic shakedown of 3D periodic heterogeneous media: a direct numerical approach. *Int J Plast* 2004;20:1655–75.
- [36] Bisbos CD, Makrodimitropoulos A, Pardalos P. Second-order cone programming approaches to static shakedown analysis in steel plasticity. *Optim Meth Soft* 2005;20:25–52.
- [37] Nguyen AD, Hachemi A, Weichert D. Application of the interior point method to shakedown analysis of pavements. *Int J Numer Meth Eng* 2008;4:414–39.
- [38] Hachemi A, Mouhtamid S, Nguyen A, Weichert D. Application of shakedown analysis to large-scale problems with selective algorithm. In: Weichert D, Ponter A, editors. *Limit states of materials and structures*. Springer; 2009. p. 289–305.
- [39] Tran TN, Liu GR, Nguyen-Xuan H, Nguyen-Thoi T. An edge-based smoothed finite element method for primal–dual shakedown analysis of structures. *Int J Numer Meth Eng* 2010;82:917–38.
- [40] Simon JW, Weichert D. Numerical lower bound shakedown analysis of engineering structures. *Comput Methods Appl Mech Eng* 2011;200:2828–39.
- [41] Zhou S, Liu Y, Wang D, Wang K, Yu S. Upper bound shakedown analysis with the nodal natural element method. *Comput Mech* 2014;54:1111–28.
- [42] Le CV, Tran TD, Pham DC. Rotating plasticity and nonshakedown collapse modes for elastic–plastic bodies under cyclic loads. *Int J Mech Sci* 2016;111:55–64.
- [43] Yamaguchi T, Kanno Y. Ellipsoidal load-domain shakedown analysis with von Mises yield criterion: a robust optimization approach. *Int J Numer Meth Eng* 2016;107:1136–44.
- [44] Cecot W. Application of h-adaptive FEM and Zarka's approach to analysis of shakedown problems. *Int J Numer Meth Eng* 2004;61:2139–58.
- [45] Krabbenhöft K, Lyamin AV, Sloan SW. Bounds to shakedown loads for a class of deviatoric plasticity models. *Comput Mech* 2007;39:879–88.
- [46] Chen HF, Ponter ARS. Shakedown and limit analyses for 3-D structures using the linear matching method. *Int J Press Vess Pip* 2001;78:443–51.
- [47] Ponter ARS. Shakedown limit theorems for frictional contact on a linear elastic body. *Eur J Mech A/Solids* 2016;60:17–27.
- [48] Garcea G, Armentano G, Petrolo S, Casciaro R. Finite element shakedown analysis of two-dimensional structures. *Int J Numer Meth Eng* 2005;63:1174–202.
- [49] Garcea G, Leonetti L. A unified mathematical programming formulation of strain driven and interior point algorithms for shakedown and limit analysis. *Int J Numer Meth Eng* 2011;88:1085–111.
- [50] Hjiij M, Krabbenhöft K, Lyamin AV. Direct computation of shakedown loads via incremental elastoplastic analysis. *Fin Elem Anal Des* 2016;122:39–48.
- [51] Spiliopoulos KV, Panagiotou KD. A residual stress decomposition based method for the shakedown analysis of structures. *Comput Methods Appl Mech Eng* 2014;276:410–30.
- [52] Spiliopoulos KV, Panagiotou KD. A numerical procedure for the shakedown analysis of structures under thermomechanical loading. *Arch Appl Mech* 2015;85:1499–511.
- [53] Spiliopoulos KV, Panagiotou KD. RSDM-S: a method for the evaluation of the shakedown load of elastoplastic structures. In: Fuschi P, Pisano AA, Weichert D, editors. *Direct methods for limit and shakedown analysis of structures*. Springer International Publishing; 2015. p. 159–75.
- [54] Panagiotou KD, Spiliopoulos KV. Assessment of the cyclic behavior of structural components using novel approaches. *ASME J Press Vess Tech* 2016;138. 0412-01-041201-10.
- [55] Simon JW, Weichert D. Shakedown analysis with multidimensional loading spaces. *Comput Mech* 2012;49:477–85.
- [56] Luenberger DG, Ye Y. *Linear and nonlinear programming*. New York: Springer; 2008.
- [57] Frederick CO, Armstrong PJ. Convergent internal stresses and steady cyclic states of stress. *J Strain Anal* 1966;1:154–69.
- [58] Polizzotto C. Variational methods for the steady state response of elastic–plastic solids subjected to cyclic loads. *Int J Solids Struct* 2003;40:2673–97.
- [59] Gokhfeld DA, Cherniavsky OF. *Limit analysis of structures at thermal cycling*. Netherlands: Sijthoff & Noordhoff; 1980.
- [60] König JA, Kleiber M. On a new method of shakedown analysis. *Bull Acad Polon Sci Ser Sci Tech* 1978;26:165–71.
- [61] Boyd S, Vandenberghe L. *Convex optimization*. Cambridge: Cambridge University Press; 2004.
- [62] Bronshtein IN, Semendyayev KA, Musiol G, Mühlhig H. *Handbook of mathematics*. 4th ed. Berlin: Springer-Verlag; 2004.
- [63] Panagiotou KD. Limit state numerical procedure for cyclically loaded elastoplastic structures [Ph.D. Dissertation]. National Technical University of Athens; 2015.
- [64] Pham PT. Upper bound limit and shakedown analysis of elastic–plastic bounded linearly kinematic hardening structure [Ph.D. Dissertation]. RWTH Aachen University; 2011.
- [65] Nijenhuis A, Wilf HS. *Combinatorial algorithms*. New York: Academic Press; 1978.
- [66] Eurocode 1. *Actions on structures*. European Union EN; 1991.
- [67] Leonetti L, Casciaro R, Garcea G. Effective treatment of complex static and dynamical load combinations within shakedown analysis of 3D frames. *Comput Struct* 2015;158:124–39.